14

Circularly Polarized Slotted/Slit-Microstrip Patch Antennas

Nasimuddin, Zhi-Ning Chen and Xianming Qing
Institute for Infocomm Research
Singapore

1. Introduction

In modern wireless communication systems, small circularly polarized microstrip antennas with good performance are desirable mainly at low microwave frequencies. The radio frequency identification (RFID) systems in the ultra-high frequency (UHF) band have gained much interest in many services [Finkenzeller2004]. The reader antenna is one of the important components in the RFID reader system and has been designed with circularly polarized (CP) radiation. The RFID system consists of the reader and the tag. Normally, the UHF tag antennas are linearly polarized. The circularly polarized microstrip antennas (CPMAs) can reduce the loss caused by the multipath effects between a reader and the tag antenna. The circularly polarized reader antenna is useful in particular when tag antenna system is in rotating motion or when its respective orientation cannot be ensured.
Total frequency span of 840 - 960 MHz is used over worldwide for UHF RFID systems. The UHF RFID system operates at the bands of 902 - 928 MHz for North-South America, 865 - 867 MHz for Europe and 840 - 955 MHz for Asia-Pacific region. The compact CPMA design to cover total UHF RFID frequency span for handheld RFID applications is very difficult. Overall sizes of the broadband CPMAs to cover woldwide RFID applications are bulky [Chen2009, Chung2007]. However these broadband antennas are not suitable for handheld or portable reader applications. Design of the compact CPMA is attractive for handheld/ portable device applications. Small size of the CPMA can be achieved at the cost of limited gain and narrow 3-dB Axial ratio (AR) bandwidth/ 10-dB return loss impedance bandwidth. A CPMA with a low-profile, small-size, and light weight is required in a portable/ handheld RFID reader. However the compact CP reader antenna should be covered at least one country frequency span used for RFID UHF band [Nasimuddin2010, Nasimuddin2009]. A typical technique for producing CP is to excite two orthogonal linearly polarized modes with a 90^{o} phase difference of the patch antenna. The single-feed CP annular-ring, square and circular microstrip patch antennas with perturbation elements have reported in [Chen1999, Chen2001, Row2004, Huang1998, Hyun2008, Row 2005, Sharma 1983]. Using perturbation or strips or slots on a radiating patch two orthogonal modes can be generated at around resonance frequency with 90^{o} phase-shift for CP radiation requirements. The single-feed circularly polarized microstrip antennas [Haneishi1988, Wong2002] are generally compact when compared with the dual-feed CPMAs [Tragonski1993]. Single-feed CPMA is simple, compact structure, easy manufacture, and low-cost. However, the single-feed conventional microstrip antennas [Sharma1983,

Haneishi1988, Wong2002, Iwasaki1996] usually have very narrow 3-dB axial-ratio bandwidth which is not suitable for many wireless communication applications such as 2.4 – 2.48 GHz. Several kinds of the radiating patch elements such as square, circular, triangular and ring shapes have been used to obtain a CP radiation using single-feed [Wong2002]. Iwasaki has been reported a proximity-coupled fed circular CPMA with a centrally located asymmetric cross-slot on a circular patch radiator. Asymmetric cross-slot provides necessary perturbation to excite two orthogonal modes with 90º phase-shift to generate CP radiation. However, 2-dB axial-ratio bandwidth of the antenna is 0.65%. For improvement of CP bandwidth, a single series feeding cross-aperture coupled microstrip antenna with effect of hybrid-feeding has been presented in [Kim2003]. However, this feeding structure needs more ground-plane size and it is not useful for compact CPMAs design. A proximity-coupled fed ring antenna was presented in [Ramirez2000] for CP radiation. CP radiation is achieved by adding two inner stubs of perturbation method. In [Tong2007], a slotted patch radiator design was proposed; in which CP radiation is achieved by using the asymmetric *U*-shaped slot embedded patch. Aperture-coupled asymmetric cross-slotted microstrip antenna can be used for CP radiation [Huang1999]. Measured 3-dB axial-ratio bandwidth of the antenna is 1.79%. Unfortunately, information on gain, overall antenna size and 3-dB AR beamwidth of the antenna is not available. Aperture-coupled fed antenna structures have attracting much attention because their geometries are suitable for monolithic integration with microwave or millimeter devices. Aperture-coupled structure is also useful for antenna array design. Nasimuddin et al. [Nasimuddin2008, 2009, 2008] have been proposed an aperture-coupled asymmetric *C*-shaped slotted microstrip antenna for CP radiation. The asymmetric *C*-shaped slotted microstrip patch is fabricated on a dielectric substrate and mounted on a thick foam substrate. Aperture-coupled fed asymmetric *S*-shaped slotted microstrip antenna can also be used for dual-band CP radiation [Nasimuddin2010].

First part of this chapter is studied on compact circularly polarized slotted/ slit-microstrip patch antennas for UHF RFID reader applications. The slotted/ slit-microstrip patch can be used for overall size reduction of the microstrip patch antenna with CP radiation. By slightly changed circumference one of diagonal slot/ slit as compared to other diagonal slot/ slit, the CP radiation of the antenna can be obtained. Performances of various slotted/ slit-microstrip antennas are also compared. The parametric studied of the *V*-shaped slits microstrip antenna is also presented to understand the generation of CP radiation. Second part of chapter is studied and comparison of the aperture-coupled fed circularly polarized slotted-microstrip patch antennas to cover frequency range 2.4 - 2.48 GHz. The antenna consists of slotted square patch and an aperture-coupled feeding structure. The asymmetric *C*-shaped, symmetric *S*-shaped and asymmetric *Z*-shaped slotted patches are fabricated from 0.5 mm copper sheet. Each slotted patch is mounted on a same size thick foam substrate. Slot dimensions are optimized for good CP radiation with fixed antenna and patch sizes. Performance of the slotted microstrip antennas are compared and studied. Design and optimization of proposed antennas were conducted with the help of commercial EM software, IE3D [IE3D2010].

2. Compact CP slotted/slit-microstrip structures and designs for RFID readers

Cross-section of the typical compact circularly polarized slotted/ slit-microstrip patch antenna is shown in Figure 1. Various slotted/ slit-microstrip patches are shown in Figures

2(a) – 2(e) for CP radiation with compact antenna size. Ground-plane size of 90 mm × 90 mm is fixed for all patch radiators. Square patch length of all patch radiators is also fixed (L = 80.0 mm). The microstrip patch antennas are designed on a RO4003 substrate (H = 4.572 mm, ε_r = 3.38 and $\tan\delta$ = 0.0027). Coaxial feed location (F) from center of the microstrip patch is y_o.

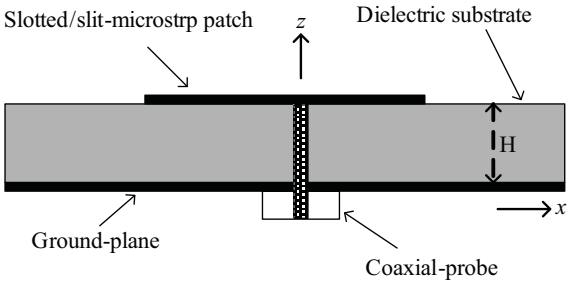

Fig. 1. Cross-section view of the proposed CP slotted/ slit-microstrip antenna.

Various slotted/ slit-microstrip patch antennas are proposed for CP radiation based on fixed overall antenna and microstrip patch sizes. All microstrip patch antennas are optimized for good CP radiation. Designed and optimized geometrical parameters (in mm) are added on microstrip patch structures. Figure 2(a) shows the conventional truncated corners microstrip patch [Sharma1983] for comparison (Antenna#1). Rectangular slot [Sharma1983] along one of the diagonal axes at the centre of the patch radiator for CP radiation is also designed as illustrated in Figure 2(b) (Antenna#2). Figure 2(c) shows the CP cross-shaped slotted microstrip patch (Antenna#3). Figure 2(d) exhibits an asymmetric- Y-shaped slotted microstrip patch for CP radiation (Antenna#4). V-shaped slits [Nasimuddin2009] are embedded symmetrically along the diagonal directions of the microstrip patch (Antenna#5) as illustrated in Figure 2(e). Locations of four V-shaped slits are located at (P, P) along diagonal directions from centre of the square microstrip patch. A_1, A_2, A_3 and A_4 are areas of the slit along the diagonal directions. Slit areas can be determined by P, d_1, and d_2. A_1 and A_3 are same as well as A_2 and A_4 are also same. For CP radiation of the patch antenna, A_1 / A_3 should be not equal to A_2 / A_4. The antenna is symmetrical along diagonal axes.

2.1 Simulated results of CP slotted/slit-microstrip antennas and comparison

Simulated return loss, axial-ratio at the boresight and gain at the boresight of the CP slotted/ slit-microstrip antennas are compared in this section. The square patch without slit/ slot is also simulated for comparison. Resonance frequency of the square patch antenna is around 977.5 MHz. Simulated return loss of the slotted/ slit CPMAs is plotted in Figure 3(a). Simulated 10-dB return loss bandwidth is 3.13% for truncated corners microstrip antenna, 2.5% for rectangular slotted microstrip antenna, 1.80% for asymmetric-cross shaped slotted microstrip antenna, 1.60% for asymmetric Y-shaped slotted microstrip antenna and 1.63% for V-shaped slits microstrip antenna. Note that the conventional truncated corners microstrip antenna resonance frequency is higher than that of the square patch antenna resonance frequency. So that the truncated corners method is not useful for compact CPMAs designs. The V-shaped slits CP microstrip antenna exhibits the lowest resonance frequency.

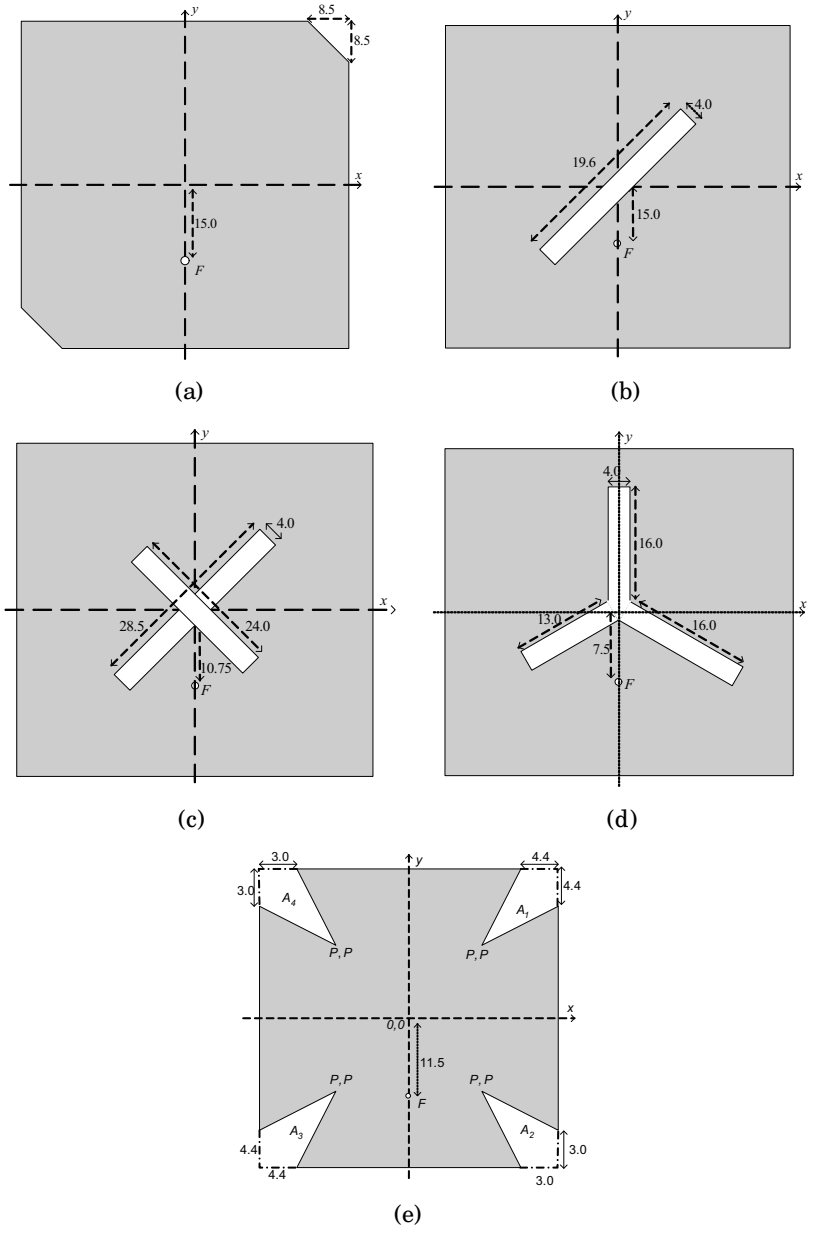

Fig. 2. Slotted/ slit-microstrip patch structures for CP; (a) Antenna#1, (b) Antenna#2, (c) Antenna#3, (d) Antenna#4 and (e) Antenna#5.

It means *V*-shaped slits microstrip antenna is electrically small when compared with the other CPMAs. Figure 3(b) shows AR of the slotted/ slit CPMAs at the boresight. Simulated 3-dB AR bandwidths of the CP slotted/ slit-microstrip antennas are 7.4 MHz (980.0 – 987.4 MHz), 6.3 MHz (960.7 – 967 MHz), 5.0 MHz (934.0 – 939.0 MHz), 4.2 MHz (922.6 – 926.8 MHz) and 5.0 MHz (917.0 – 921.0 MHz), respectively. The 3-dB AR bandwidth of truncated corners patch antenna is larger when compared to the other CPMAs.

Simulated 3-dB AR bandwidth of the *V*-shaped slits and *Y*-shaped slotted microstrip antennas are slightly narrow because these antennas are electrically small. Simulated gain at

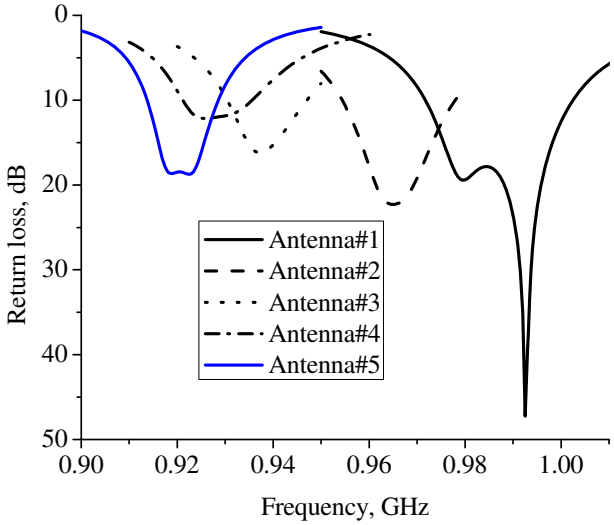

(a)

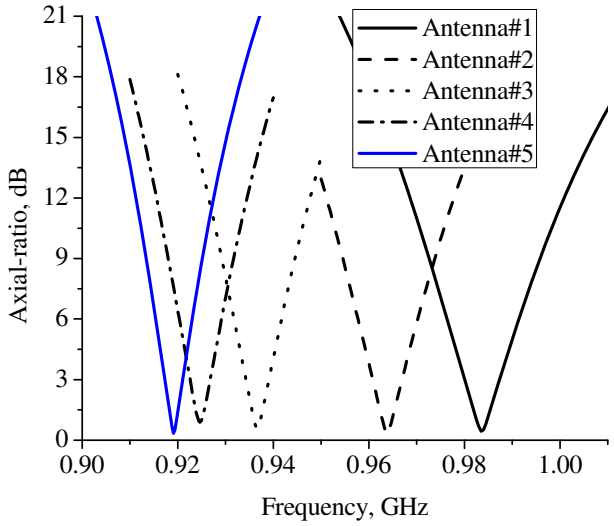

(b)

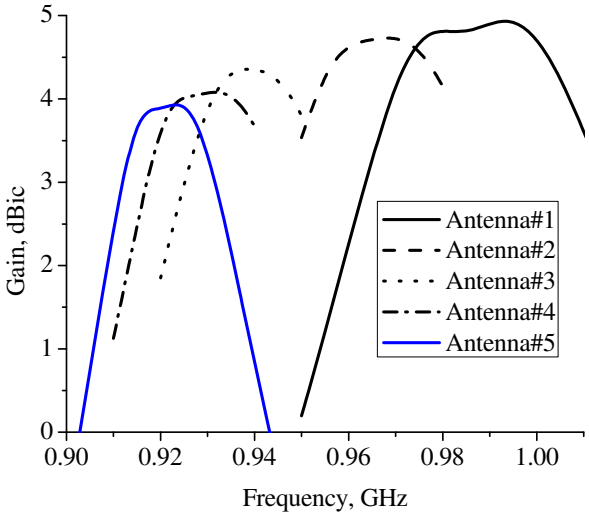

(c)

Fig. 3. Simulated performances of the CP slotted/ slit-microstrip antennas; (a) return loss, (b) axial-ratio at the boresight and (c) gain at the boresight.

the boresight of the CPMAs is compared in Figure 3(c). Broadside gain is more than 4.0 dBic for all slotted/ slit CPMAs over the 3-dB AR bandwidth except *V*-shaped slits CPMA. Gain of the *V*-shaped slits microstrip antenna is bit lower due to the antenna is electrically smallest. For RFID handheld reader applications, the small antenna size is more important. Broesight gain variation over the 3-dB AR bandwidth is less than 0.2 dB for CP slotted/ slit-microstrip antennas. Simulated performances of the CP slotted/ slit-microstrip antennas are also summarized in Table 1.

Antenna	3-dB AR frequency range (MHz)	3-dB AR bandwidth (MHz)	10-dB return loss bandwidth (%)	Gain (dBic) (maximum)
1	980.0 – 987.4	7.4 MHz	3.13% (30.0 MHz)	4.8
2	960.7 – 967.0	6.3 MHz	2.5% (24.0 MHz)	4.6
3	934.0 – 939.0	5.0 MHz	1.81 % (16.8 MHz)	4.3
4	922.6 – 926.8	4.3 MHz	1.60% (14.5 MHz)	4.1
5	917.0 – 921.0	5.0 MHz	1.63% (15.0 MHz)	3.9

Table 1. Simulated Performance of the CP Slotted/ slit-microstrip Antennas

2.2 Parametric study of slit-microstrip antenna

Parametric analysis of the circularly polarized slit-microstrip antenna (Antenna#5) is conducted to understand effect of slit parameters on the antenna performance. By changing the slit parameters, the two-orthogonal modes with 90° phase shift can be generated for requirements of circularly polarized radiation. For single-feed microstrip antenna, the orthogonal mode resonant frequencies should be much closed to get the good CP radiation. In this study, locations of the *V*-shaped slits and feed-location are fixed (P = 15.5 mm, 11.5 mm). d_2 is also fixed as 3.0 mm. By decreasing or increasing d_1 with respect to d_2, the antenna can be optimized for CP radiation. Simulated return loss, AR and gain at the boresight of the CPMA with different d_1 are plotted in Figures 4(a), (b) and (c), respectively. The d_1 is

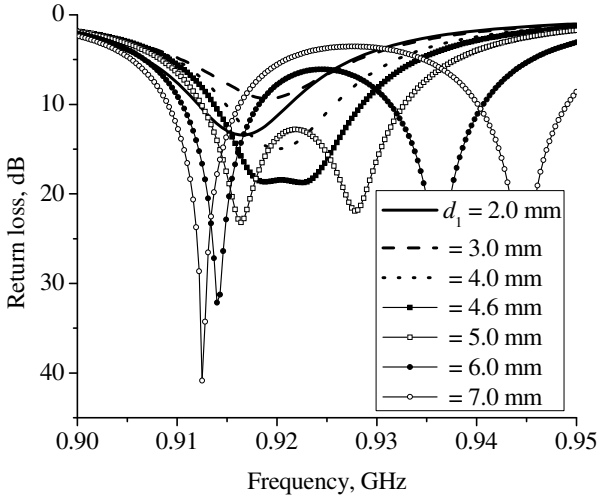

(a)

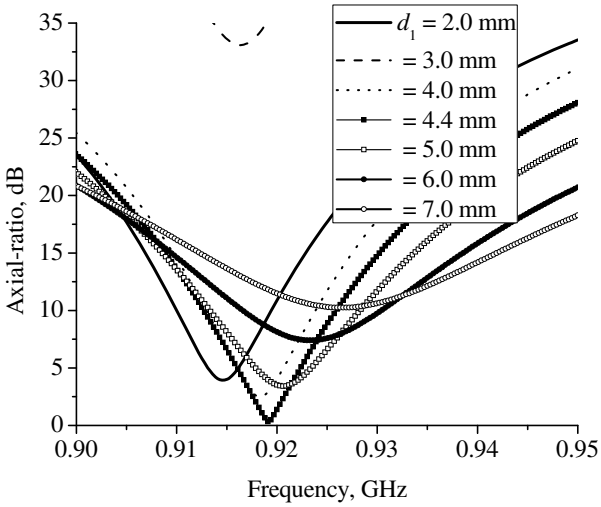

(b)

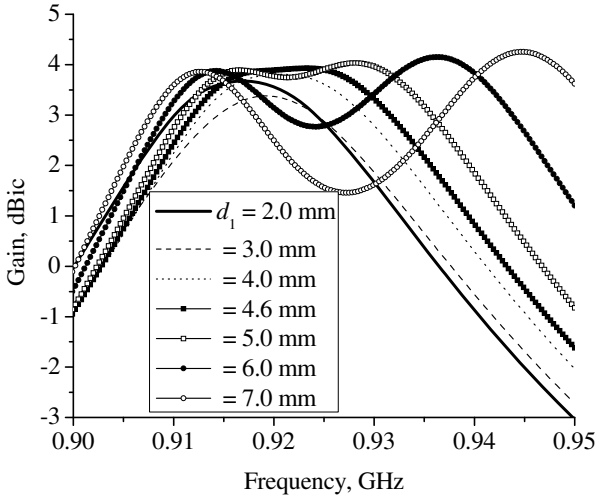

(c)

Fig. 4. Effect of the d_1 on antenna parameters: (a) return loss, (b) axial-ratio at the boresight and (c) gain at the boresight.

changed from 2.0 mm to 7.0 mm. When d_1 increases, the impedance bandwidth is enhanced while the frequency-band is moved down. Two orthogonal modes start to regenerate when d_1 increases and at around d_1 = 4.4 mm two orthogonal modes with their resonance frequencies nearly close to each other. It can be observed that the boresight AR decreases with an increase in d_1 up to 4.4 mm and then start increase AR with increases in d_1. Best AR performance is achieved, when d_1 is around 4.4 mm. When d_1 is 3.0 mm, the patch antenna with symmetric *V*-shaped slits is linear polarized radiation ($d_1 = d_2$). The axial-ratio is more than 30 dB at $d_1 = d_2$ = 3.0 mm. Boresight gain and gain bandwidth increases with increase in d_1. At around d_1 = 4.4 mm, the gain is also more flat.

2.3 Measured results and discussions of the slit-microstrip antenna

The compact circularly polarized *V*-shaped slits microstrip patch antenna was fabricated and tested. Antenna performances were measured by an Agilent vector network analyzer N5230A and MiDas 5 antenna test system. Measured 10-dB return loss bandwidth is 19.0 MHz (914 – 933 MHz). Measured 3-dB AR bandwidth is achieved around 6.0 MHz (920 – 926 MHz) and it is within the measured 10-dB return loss bandwidth. Measured maximum boresight gain is around 3.6 dBic at 921 MHz. Boresight gain remains relatively constant around 3.4 dBic with variation of less than 0.2 dB within the 3-dB AR bandwidth. Measured results on return loss, AR and gain agree well with simulated results.

Radiation patterns were measured using a rotating linear polarized transmitting horn antenna for both (*x-z* and *y-z*) principal planes. Figure 5 shows the measured radiation patterns *x-z* and *y-z* planes at 924 MHz. In both planes (*x-z* and *y-z*), the AR is found to be less than 3-dB across a 100º beamwidth over the 3-dB AR bandwidth frequency range. Proposed antenna is compact and very useful for RFID handheld reader applications. For validation of RFID reader applications of the antenna, the tag reading-range was measured for the antenna. The MP9320 2.8 EPC™ UHF reader and home made UHF tag were used for

the measurement of the reading range. The maximum reading range of 60 – 65 cm is achieved at the boresight.

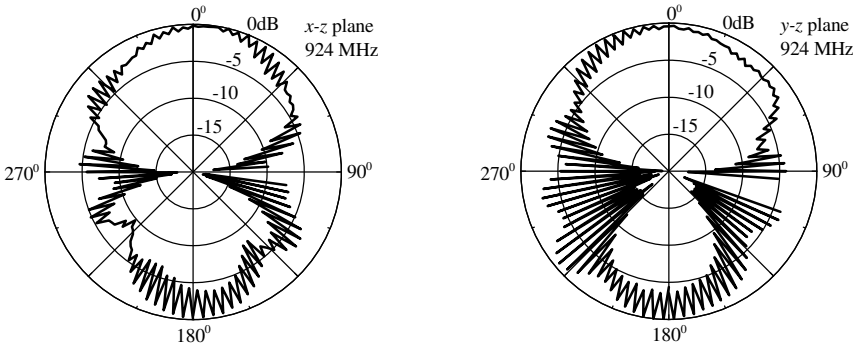

Fig. 5. Measured radiation patterns at 924 MHz.

2.4 Symmetric-slit with slot based compact CP microstrip antennas

In this section, the symmetric-slit microstrip patch based compact circularly polarized microstrip antennas are also designed at frequency around 2.4 GHz. The slit-slotted microstrip patch radiators are printed on the RO4003C substrate (H = 1.524 mm, ε_r = 3.38 and $tan\delta$ = 0.0027). The square patch (L) and ground-plane sizes are 31.8 mm and 36.0 mm × 36.0 mm, respectively. The coaxial feed-location (y_o) is 5.0 mm from centre of the patch radiator. Designed dimensions of the patch radiators are shown in patch sketches.

The V-shaped symmetric-slit along with circular slot at the centre of square patch radiator is shown in Figure 6. The circularly polarized radiation is achieved by changing the area of slits along the diagonal directions ($A_1 > A_2$). Simulated resonance frequency of the square patch without slits and slot is around 2.488 GHz. The measured and simulated return loss is

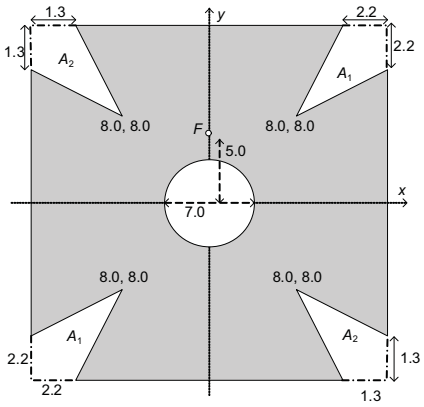

Fig. 6. Symmetric-slit with circular-slot patch radiator.

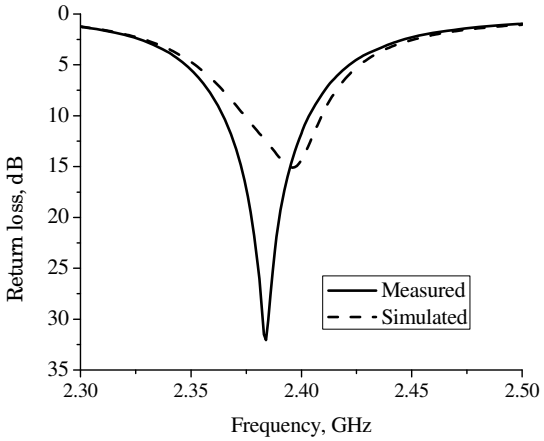

Fig. 7.(a). Simulated and measured return loss of the symmetric-slit patch with circular slot.

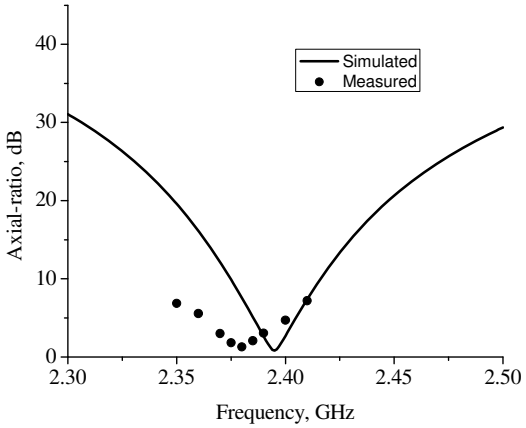

Fig. 7.(b). Simulated and measured axial-ratio at the boresight

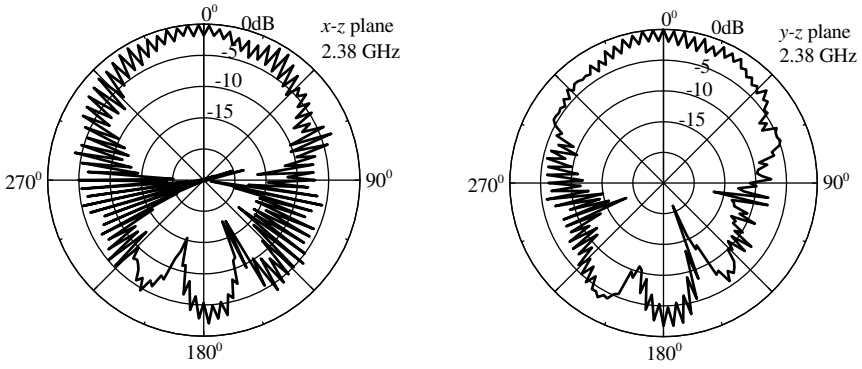

Fig. 8. Measured radiation patterns in *x-z* and *y-z* planes at 2.38 GHz

plotted in Figure 7(a). Measured resonance frequency of the proposed slit-slotted microstrip patch antenna is 2.384 GHz. Boresight minimum axial-ratio is around the 2.38 GHz as shown in Figure 7(b). Simulated and measured results are good agreement. The boresight measured gain is more than 3.5 dBic over the 3-dB AR bandwidth. Measured radiation patterns in *x-z* and *y-z* planes at 2.38 GHz are plotted in Figure 8. Operating frequency of the antenna is lower when compared with the square patch antenna. As a result the slit-slotted microstrip antenna is electrically small.

Other *V*-shaped symmetric-slit along with rectangular slot in diagonal direction at the centre of square patch radiator is shown in Figure 9. The circularly polarized radiation is achieved using rectangular slot along the diagonal direction at centre of the patch. Note that the area of slits along the diagonal directions are same in this antenna ($A_1 = A_2$). The measured and simulated results on return loss and axial-ratio at the boresight of the antenna are illustrated in Figures 10(a)-(b), respectivily. The measured 10-dB return loss bandwidth is 2.34 – 2.38 GHz. The centre frequency is around 2.36 GHz and minimum axial-ratio is achieved at around 2.355 GHz. The proposed symmetric-slit with slotted microstrip antennas are compact when compared with the conventional square patch antenna. Resonance frequency of the symmetric-slit with rectangular-slot microstrip patch antenna is lowest when compared with the circular-slot and conventional square patch antennas. The measured spining radiation pattrens at x-z and y-z planes are plotted in Figure 10(c).

3. Aperture-coupled slotted-microstrip structures

Cross-section view of the typical aperture-coupled fed CP slotted microstrip antenna is shown in Figure 11(a). The slotted patch radiators (asymmetric *C*-shaped [Nasimuddin2008, Nasimuddin2009], symmetric *S*-shaped and asymmetric *Z*-shaped) are illustrated in Figures 11(b)-11(d). Length of a square microstrip patch is *L*. *H* is the total antenna height and h_2 is the foam thickness. The 50-Ω microstrip feed-line and the coupling aperture are printed on the opposite surfaces of the RO4003C substrate (h_1 = 1.524 mm, ε_{r1} = 3.38 and $tan\delta_1$ = 0.0027). Microstrip feed-line from center of an aperture is S_f as shown in Figure 11(e). W_a is aperture width and L_a is aperture length. Aperture-coupled feed is located at center of the slotted

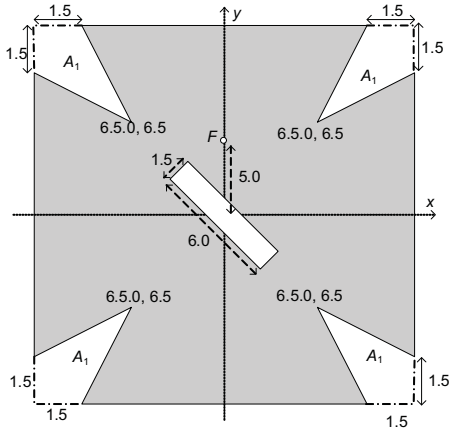

Fig. 9. *V*-shaped symmetric-slit with rectangular-slot patch radiator.

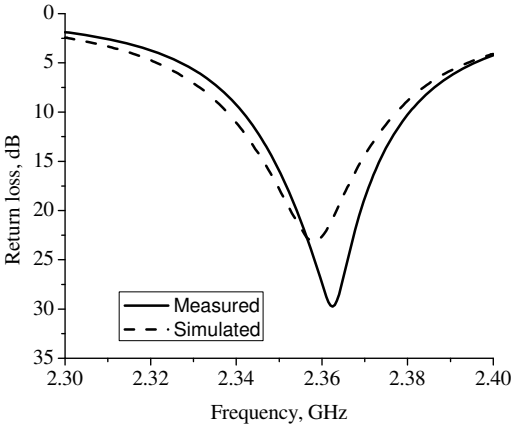

Fig. 10. (a). Simulated and measured return loss of the symmetric-slit with rectangular slot patch antenna.

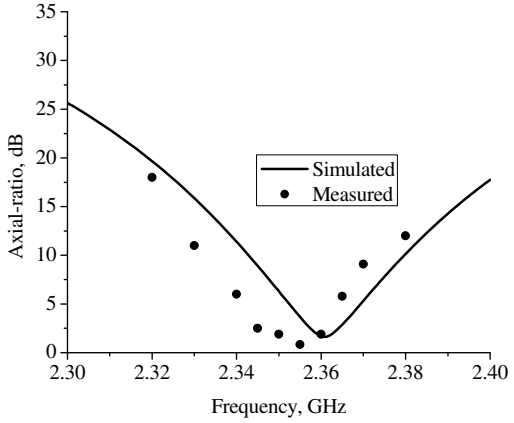

Fig. 10. (b). Simulated and measured axial-ratio at boresight of the symmetric-slit with rectangular slot patch antenna.

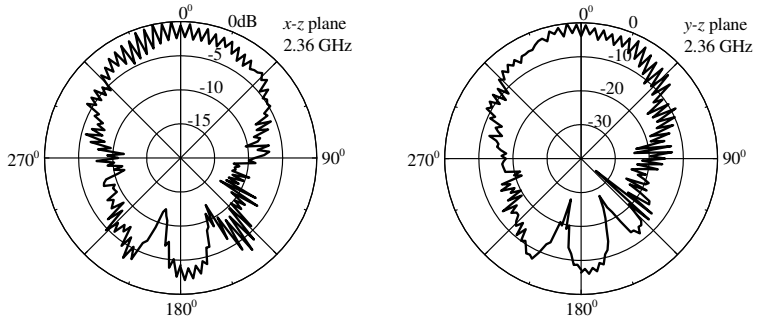

Fig. 10. (c). Measured radiation patterns in *x-z* and *y-z* planes at 2.36 GHz of the symmetric-slit with rectangular slot patch antenna

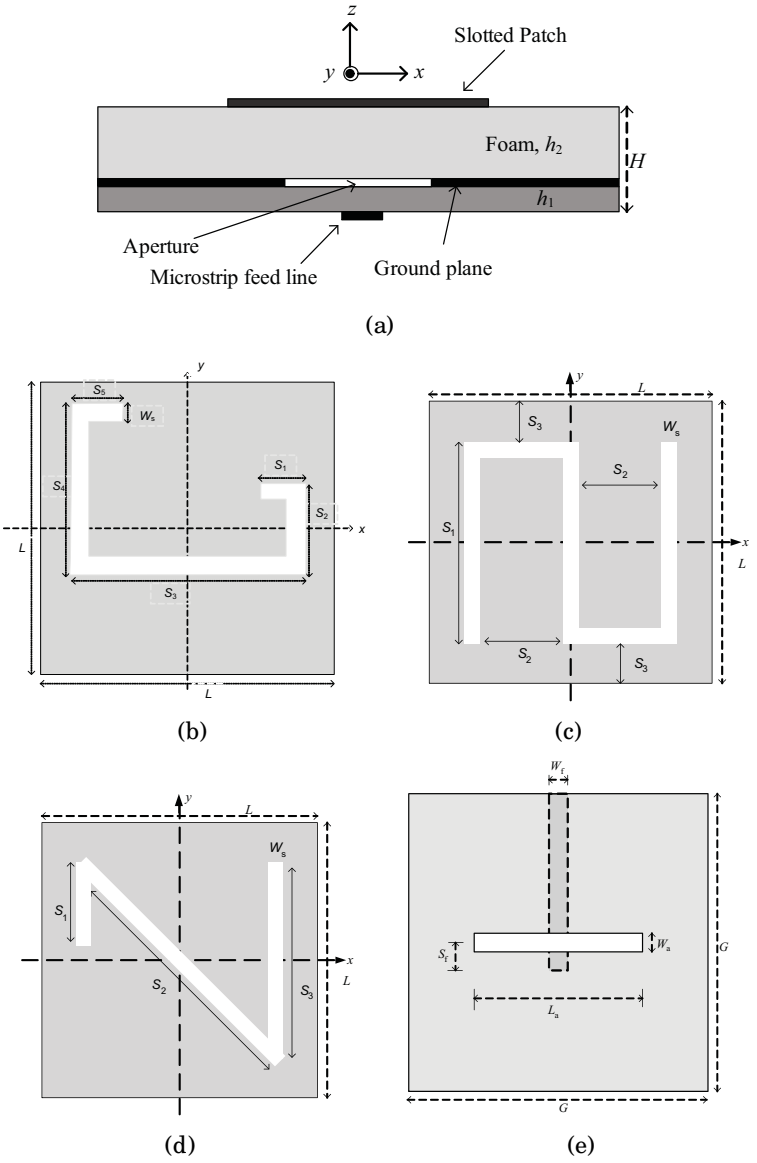

Fig. 11. Aperture-coupled CP slotted microstrip antenna; (a) cross-section view, (b) *C*-shaped slotted patch, (c) *S*-shaped slotted patch, (d) *Z*-shaped slotted patch, and (e) aperture-coupled feed structure.

square radiator. The slotted patch radiator can cause meandering of excited surface current paths and result in lowering resonance frequency. As a result electrical size of the antenna is reduced. By adjusting the slot size, the two near-degenerated resonance modes with 90° phase-shift can be generated for CP radiation of the slotted square patch antenna. Lengths of the slot can be used to optimize the antenna for minimum AR, wide AR bandwidth, wide impedance bandwidth and size reduction. Three sets of the slot shapes are selected and optimized for minimum AR, wide CP bandwidth and compact antenna size with help of [Nasimuddin2008-2010] based on same antenna and patch radiator sizes. Optimized dimensions of the slots are given in Table 2 and all dimensions are in mm.

Parameters	*C*-shaped slot	*S*-shaped slot	*Z*-shaped slot
L	43.0	43.0	43.0
Ground plane ($G \times G$)	60.0 × 60.0	60.0 × 60.0	60.0 × 60.0
W_s	3.0	3.0	3.0
S_1	3.5	30.0	12.5
S_2	8.0	13.5	42.5
S_3	28.0	6.50	33.1
S_4	21.0	-	-
S_5	5.5	-	-
S_f	4.0	4.0	4.0
W_a	33.0	33.0	33.0
L_a	3.0	3.0	3.0
H	11.524	11.524	11.524

Table 2. Designed and optimized dimensions of the slotted microstrip antennas.

3.1 Comparison of aperture-coupled CP slotted microstrip patch antennas

In this section, three types of the slotted patch radiators are studied by simulation for good CP radiation with fixed antennas size. Simulated return loss, AR at the boresight and gain at the boresight of the slotted microstrip patch antennas are studied and compared. Return loss of the slotted microstrip antennas are plotted in Figure 12(a). Simulated 10-dB return loss bandwidth is around 13.5% (2.230 – 2.554 GHz) for asymmetric *C*-shaped slotted patch, 14.0% (2.092 – 2.407 GHz) for symmetric *S*-shaped slotted patch and 14.2% (2.188 – 2.522 GHz) for asymmetric *Z*-shaped slotted patch. Impedance bandwidth of the asymmetric *Z*-shaped slotted antenna is larger. Figure 12(b) shows axial-ratio at the boresight of the slotted antennas. Simulated 3-dB axial-ratio bandwidths of the asymmetric *C*-shaped, symmetric *S*-shaped and asymmetric *Z*-shaped slotted antennas are 3.1% (2.406 – 2.483 GHz), 2.1% (2.250 – 2.310 GHz) and 2.62% (2.409 – 2.473 GHz), respectively. Minimum AR is 0.72 dB at 2.445 GHz for asymmetric *C*-shaped slot, 0.14 dB at 2.267 GHz for symmetric *S*-shaped slot and 0.64 dB at 2.445 GHz for asymmetric *Z*-shaped slot. Simulated gain at the boresight of the slotted antennas is compared in Figure 12(c). Boresight gain is more than 6.0 dBic for all antennas over the impedance bandwidth. Gain variation with frequency over the impedance bandwidth is less than 0.5 dB for all antennas. Lowest resonance frequency of the antenna is

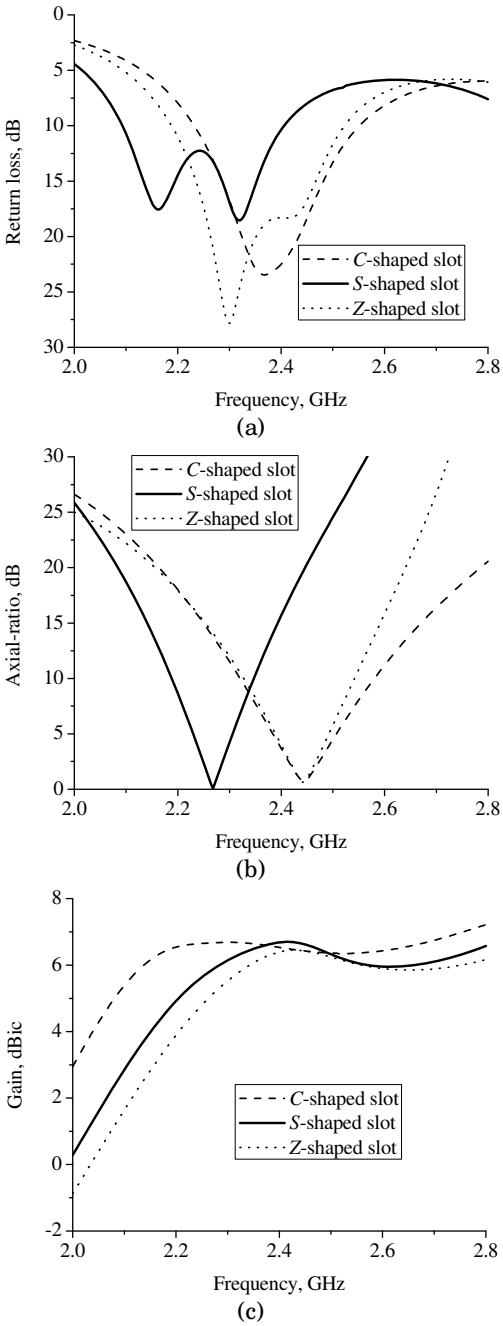

Fig. 12. Simulated results of the slotted microstrip antennas; (a) return loss, (b) axial-ratio at the boresight and (c) gain at the boresight.

achieved with symmetric *S*-shaped slotted patch. The symmetric *S*-shaped slotted antenna has 7% overall area reduction when compared with the asymmetric *C*-shaped and *Z*-shaped slotted microstrip antennas. However, its the 3-dB axial-ratio bandwidth is narrow when compared with the asymmetric *C*- and *Z*-shaped slotted antennas. Minimum axial-ratio dip frequency for the asymmetric *C*- and *Z*-shaped slotted patch is almost same. The symmetric *S*-shaped slotted patch is useful for compact CP microstrip antenna design. For wide CP bandwidth CPMA design, the asymmetric *C*-shaped slotted patch radiator is better.

3.2 Parametric study of aperture-coupled Z-shaped slotted microstrip antenna

In this section, the parametric studied is conducted of the *Z*-shaped slotted microstrip patch antenna. The S_1 arm of *Z*-shaped slot is varied to study the CP radiation generation for *Z*-shaped slotted patch antenna and variation of antenna performances. The return loss, axial-ratio at the boresight and gain at the boresight with variation of S_1 are plotted in Figures 13(a)-(c) respectively. The 10-dB return loss bandwidth increases with decrease in S_1 of *Z*-shaped slot and starts degenerate two orthogonal modes with 90° phase-shift for CP radiation requirements. At around S_1 = 12.5 mm, lowest axial-ratio can be achieved for good CP radiation. The axial-ratio decreases with increase in S_1 as shown in Figure 13(b). The brosight gain is not significant effect with variation of S_1 as plotted in Figure 13(c).

The current distributions of the slotted patch antennas are shown in Figures 14(a) - (c), respectively. Strongest current distribution is at around asymmetric *C*-shaped slot arm S_6 as shown in Figure 14(a). These current distributions are at minimum axial-ratio frequencies of the antennas. The S_6 is very sensitive to optimize the *C*-shaped slotted antenna for best CP (minimum AR) and wide CP bandwidth. Strongest current distribution is at around symmetric *S*-shaped slot. The symmetric *S*-shaped slotted radiating patch can cause meandering of the excited patch surface current paths is more when compared with the asymmetric *C*-shaped and *Z*-shaped slotted patches as shown in Figure 14(b). Lowering resonance frequency of the antenna, which is corresponds to a reduced antenna size for such a fixed overall antenna size. For left hand CP radiation, S_2 should be greater than S_4 (*C*-shaped slotted patch), S_1 should be greater than S_3 (*Z*-shaped slotted patch), and for the right hand CP radiation, S_2 should be less than S_4 (*C*-shaped slotted patch), S_1 should be less than S_3 (*Z*-shaped slotted patch). For changing the polarization sense of the *S*-shaped slot patch antenna, *S*-shaped slot should be rotated by 180° with respect to feed axis.

3.3 Measured results and discussions of the slotted-microstrip antennas

Optimized aperture-coupled fed slotted patch antennas are fabricated and tested. The slotted patch radiators are fabricated from 0.5 mm thick copper sheet and each mounted on a thick foam substrate of height (h_2 = 10 mm). Measured performance of the aperture-coupled slotted patch antennas is summarized in Table 3. The asymmetric *C*-shaped slotted patch antenna has larger CP bandwidth (3-dB axial-ratio bandwidth) when compared with the symmetric *S*-shaped and asymmetric *Z*-shaped slotted antennas. The symmetric *S*-shaped slotted patch antenna is electrically small when compared with the asymmetric *C*- and *Z*-shaped slotted patch antennas. The slotted patch antennas have a wide angle CP of more than 90°. Measured performance of the slotted patch antennas is also compared with some related structures in the published literatures. The slotted patch antennas are compact and have large impedance bandwidth when compared with the other published antennas. All three *C*-, *S*-, and *Z*-shaped slotted patch antennas show overall antenna size is less than

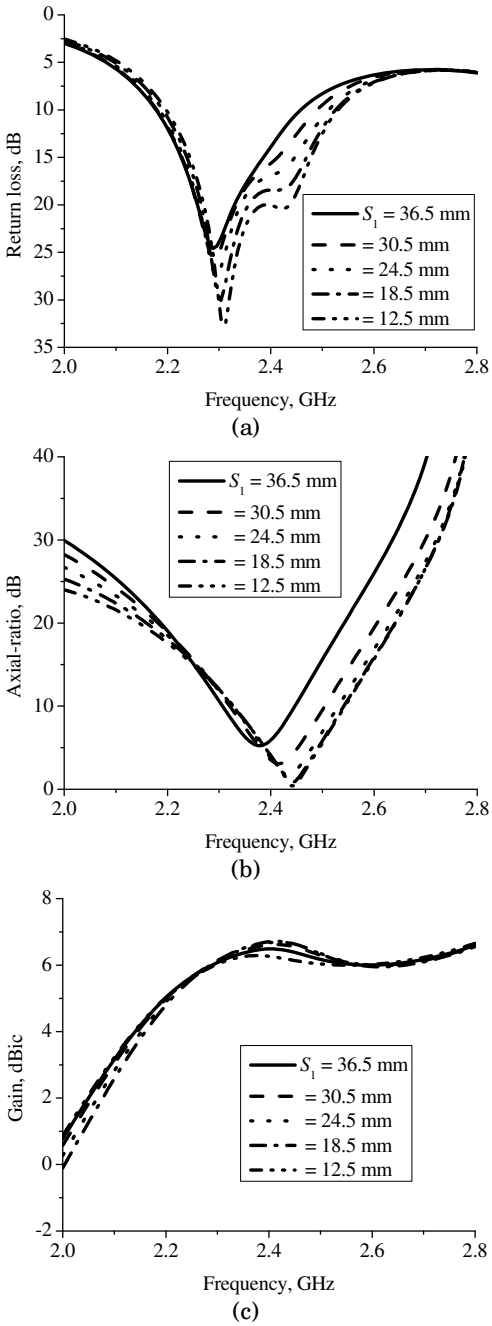

Fig. 13. Effect of the S_1 on antenna parameters of Z-shaped slot antenna; (a) return loss, (b) axial-ratio at the boresight and (c) gain at the boresight.

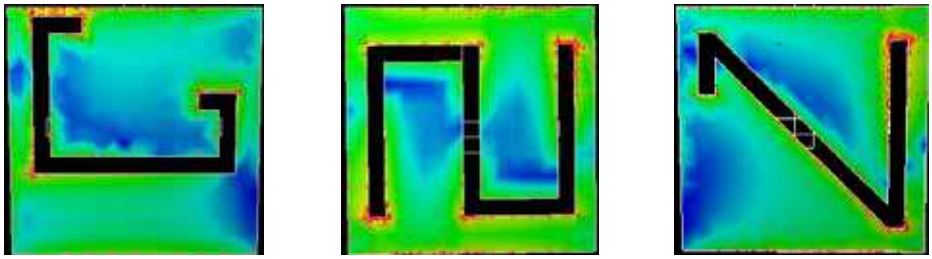

(a) (b) (c)

Fig. 14. Current distributions on the slotted patch radiators with slots; (a) *C*-shaped slot, (b) *S*-shaped slot and (c) *Z*-shaped slot.

Antenna structures	Overall antenna size	3-dB Beamwidth	3-dB AR bandwidth (%)	10-dB return loss bandwidth (%)
C-shaped slot	$0.48\lambda_o \times 0.48\lambda_o \times 0.092\lambda_o$ at 2.40 GHz	$> 90^o$	3.31	14.9
S-shaped slot	$0.45\lambda_o \times 0.45\lambda_o \times 0.087\lambda_o$ at 2.25 GHz	$> 90^o$	2.50	13.5
Z-shaped slot	$0.48\lambda_o \times 0.48\lambda_o \times 0.0927\lambda_o$ at 2.40 GHz	$> 90^o$	2.85	14.7
F-shaped slot [Yeh2009]	$0.533\lambda_o \times 0.533\lambda_o \times 0.0815\lambda_o$ at 2.45 GHz	$> 90^o$	4.8	14.4
U-shaped slot [Tong2007]	$0.785\lambda_o \times 0.785\lambda_o \times 0.108\lambda_o$ at 2.30 GHz	58^o	4.0	9.0
[Huang1999]	-	-	1.25	3.93

Table 3. Measured performances of the antennas.

half wavelength in free space. The asymmetric *U*-shaped slot antenna [Tong2007] has narrow angle CP when compared with the *C*, *S*, *Z* and *F*-shaped slotted patch antennas. The aperture-coupled asymmetric *S*-shaped antenna has electrically smallest antenna size. However, the *F*-shaped slotted microstrip antenna [Yeh2009] has largest 3-dB AR bandwidth. The 10-dB return loss bandwidth and 3-dB beamwidth of the *C*, *S*, *Z* and *F*-shaped slotted microstrip antennas are almost same. The *U*-shaped slotted patch antenna has lower impedance bandwidth due to this antenna is coaxial feed.

4. Conclusion

The compact CP slit/ slotted-microstrip antennas have been presented for UHF RFID handheld reader applications. Various slotted/ slit-microstrip patches have also been studied and compared with fixed antenna size. It has been found that the slotted-slit-microstrip patch radiator can be used for small overall size CPMA design. The presented CPMAs have wide angle CP (3-dB AR beamwidth) of more than 100^o over the 3-dB AR frequency range. A parametric study of the *V*-shaped slit-microstrip antenna has been

conducted. It has also been found that the impedance matching and AR can be optimized easily by adjusting the slit sizes. This chapter has been also presented the aperture-coupled circularly polarized slotted patch antennas. Small overall size of the antenna is achieved with symmetric *S*-shaped slotted microstrip patch. Symmetric *S*-shaped slotted patch radiator is better choice for the compact CPMA design. The *F*-shaped slotted patch antenna has larger 3-dB AR bandwidth. The slotted patch antennas have a wide angle CP radiation (3-dB AR beamwidth) of more than 90^{o} over the 3-dB axial-ratio frequency range. The proposed combined slotted-slit patch technology is useful for compact CPMAs and array designs.

5. Acknowledgment

The authors wish to thank T. M. Chiam for fabrication of the antenna prototypes, C. K. Goh for helping in measurement of reading range of the reader antenna.

6. References

Finkenzeller, K. (2004). *RFID Handbook*, Wiley, 2nd edition, New York, USA

Chen, Z.N., Qing, X., and Chung, H.L. (May2009). A universal UHF RFID reader antenna", *IEEE Trans Microwave Theory and Techniques*, Vol 57, No.5, 2009, pp. 1275-1282

Chung, H.L., Qing, X., Chen, Z. N. (2007). Broadband circularly polarized stacked probe-fed patch antenna for uhf RFID applications, *International Journal of Antennas and Propagation*, Vol. 2007, pp. 1-9

Nasimuddin, Chen, Z.N. and Qing, X. (December2010), Asymmetric-circular shaped slotted microstrip antennas for circular polarization and RFID applications, *IEEE Trans. Antennas and Propagation*, Vol.58, No.12, pp.3821-3828, 2010

Nasimuddin, Qing, X. and Chen, Z.N. (December2009), Compact circularly polarized microstrip antenna for RFID handheld reader applications, *Asia Pacific Microwave Conference,* December 2009, Singapore, pp. 1950-1953.

Chen, H.M., and Wong, K.L. (August1999), On the circular polarization operation of annular-ring microstrip antennas, *IEEE Trans. Antennas and Propagation*, 1999, Vol.47, No.8, pp. 1289–1292

Chen, W.S., Wu, C.K., and Wong, K.L. (March2001), Novel compact circularly polarized square microstrip antenna, *IEEE Trans. Antennas Propagation*, 2001, Vol.49,No.3, pp. 340–342

Row, J.S., and Ai, C.Y.(2004), Compact design of single-feed circularly polarized microstrip antenna, *Electronics Letters*, 2004, Vol.40, No.18, pp. 1093–1094

Huang, C.Y., Wu, J.Y., and Wong, K.L.(1998), Slot-coupled microstrip antenna for broadband circular polarization, *Electronics Letters*, 1998, Vol.34, No.9, pp. 835–836

Hyun, D.H., Baik, J.W., and Kim, Y.S.(2008), Compact reconfigurable circularly polarized microstrip antenna with asymmetric cross slots, *Microwave and Optical Technology Letters*, 2008, Vol.50, No.8, pp. 2217–2219

Row, J.S. (May 2005), Design of aperture-coupled annular-ring microstrip antenna for circular polarization, *IEEE Trans. Antennas and Propagation*, 2005, Vol.53, No.5, pp. 1779–1784

Sharma, P.C., and Gupta, K.C.(June 1983), Analysis and optimized design of single feed circularly polarized microstrip antennas, *IEEE Trans. Antennas and Propagation*, 1983, Vol. 29, No.6, pp. 949–955

Haneishi, M., and Yoshida, S.(1988), A design method of circularly polarized rectangular microstrip antenna by one-point feed, Microstrip Antenna Design, K.C. Gupta and A. Benalla (Eds), Artech House, Norwood, MA, USA, 1988, pp. 313-321

Wong, K.L.(2002), Compact circularly polarized microstrip antennas, Chapter Five, Compact and broad band Microstrip Antenna, John Wiley & Sons, Inc, USA, 2002, pp. 162-220

Targonski, S. D., and Pozar, D.M.(February 1993), Design of wideband circularly polarized aperture-coupled microstrip antennas, *IEEE Transactions on Antennas and Propagation*, February 1993, Vol.41, No.2, pp. 214-219

Iwasaki, H.(October 1996), A circularly polarized small size microstrip antennas with cross slot, *IEEE Trans. Antennas and Propagation*, Vol.44, No.10, 1996, pp. 1399 – 1401

Kim, H., Lee, B.M., and Yoon, Y.J. (2003), A single feeding circularly polarized microstrip antenna with the effect of hybrid feeding, *IEEE Antennas and Wireless Propagation Letters*, Vol.2, 2003, pp. 74-76

Ramirez, R.R., Flaviis, F.D., and Alexopoulos, N.G.(July 2000), Single-feed circularly polarized microstrip ring antenna and arrays, *IEEE Trans. Antennas and Propagation*, Vol.48, No.7, July 2000, pp. 1040-1047

Tong, K.F. and Wong, T.P.(August 2007), Circularly polarized *U*-slot antenna, *IEEE Trans. Antennas and Propagation*, Vol.55, No.8, 2007, pp. 2382-2385

Huang, C.Y.(February 1999), Design for an aperture-coupled compact circularly polarized microstrip antenna, *IEE Proc. Microwaves, Antennas and Propagation*, Vol.146, No.1, Feb. 1999, pp. 13-16

Nasimuddin, Chen, Z.N. and Qing, X.(December 2008), Single fed circularly polarized microstrip antenna with C-slot, *APMC Asia Pacific Microwave Conference* 2008, December 16-20 2008, Hong Kong/ Macau, pp. 1-4

Nasimuddin and Chen, Z.N.(April 2009), Aperture-coupled asymmetrical *C*-shaped slot microstrip antenna for circular polarization, *IET Microwaves, Antennas and Propagation*, Vol.3, No.3, April 2009, pp. 372-378

Nasimuddin, Chen, Z.N. and Qing, X.(December 2008), Aperture-coupled *C*-shape slot cut square microstrip antenna for circular polarization, *Microwave and Optical Technology Letters*, Vol.50, No.12, Dec 2008, pp. 3175-3178

Nasimuddin, Chen, Z.N. and Qing, X.(June 2010), Dual-band circularly polarized *S*-shaped slotted patch antenna with a small frequency-ratio, *IEEE Trans. Antennas and Propagation*, Vol.58, No.6, June 2010, pp. 2112-2115

IE3D EM simulator, version 14.0, 2010.

Yeh,Y., Nasimuddin, Chen, Z.N. and Alphones, A.(April 2009), Aperture-coupled circularly polarized *F*-slot microstrip antenna, *Microwave and Optical Technology Letters*, Vol.51, No.4, April 2009, pp. 1100-1104

Microstrip Antennas

Edited by Prof. Nasimuddin Nasimuddin

ISBN 978-953-307-247-0
Hard cover, 540 pages
Publisher InTech
Published online 04, April, 2011
Published in print edition April, 2011

In the last 40 years, the microstrip antenna has been developed for many communication systems such as radars, sensors, wireless, satellite, broadcasting, ultra-wideband, radio frequency identifications (RFIDs), reader devices etc. The progress in modern wireless communication systems has dramatically increased the demand for microstrip antennas. In this book some recent advances in microstrip antennas are presented.

InTech Europe
University Campus STeP Ri
Slavka Krautzeka 83/A
51000 Rijeka, Croatia
Phone: +385 (51) 770 447
Fax: +385 (51) 686 166
www.intechopen.com

InTech China
Unit 405, Office Block, Hotel Equatorial Shanghai
No.65, Yan An Road (West), Shanghai, 200040, China
中国上海市延安西路65号上海国际贵都大饭店办公楼405单元
Phone: +86-21-62489820
Fax: +86-21-62489821